

Simulating adiabatic quantum computation with a variational approach

Giuseppe Carleo

Institute of Physics, École Polytechnique Fédérale de Lausanne (EPFL), CH-1015 Lausanne, Switzerland

Bela Bauer and Matthias Troyer

Microsoft Azure Quantum

The theoretical analysis of the Adiabatic Quantum Computation protocol presents several challenges resulting from the difficulty of simulating, with classical resources, the unitary dynamics of a large quantum device. We present here a variational approach to substantially alleviate this problem in many situations of interest. Our approach is based on the time-dependent Variational Monte Carlo method, in conjunction with a correlated and time-dependent Jastrow ansatz. We demonstrate that accurate results can be obtained in a variety of problems, ranging from the description of defect generation through a dynamical phase transition in 1D to the complex dynamics of frustrated spin-glass problems both on fully-connected and Chimera graphs.

I. INTRODUCTION

Adiabatic quantum computation (AQC) is a physics-inspired paradigm to realize computations by means of controlled quantum resources. It can be seen as an alternative to the more traditional circuit model [1], and builds on the idea of reformulating the solution to a given computational problem as the task of finding the ground state of an auxiliary, problem-dependent spin Hamiltonian. The goal of the quantum computation is then to find the requested ground-state solution by means of an adiabatic, unitary time evolution which aims at staying in the instantaneous ground-state of a conveniently designed driving Hamiltonian. The resulting computing paradigm is universal in the sense that any quantum algorithm can be reformulated in the AQC form [2, 3]. Moreover, a subset of AQC where the final target Hamiltonian is classical, commonly referred to as adiabatic quantum optimization (AQO), has enjoyed significant experimental progress in recent years [4–7], and several applications have already been put forward [8–10]. The theoretical analysis of AQC algorithms, however, is a particularly challenging task. The largest difficulties arise because of the intrinsically non-perturbative and strongly interacting nature of the Hamiltonians resulting from the AQC mapping, requiring the ability to study the unitary dynamics of an intricate many-body quantum system. As expected for a model that is universal for quantum computation, simulating these dynamics on a classical computer is exponentially difficult in the general case. Thus, exact numerical studies have been mostly confined to small systems that can be accessed with exact diagonalization [11], and theoretical efforts have been focused on understanding related problems that are more easily tractable, but still give insight into AQC. On the one hand, qualitative studies of AQO based on Quantum Monte Carlo pseudo-dynamics (simulated quantum annealing) [6, 12–14] have been realized. On the other hand, large-scale unitary dynamics has been studied for integrable models that lack frustration [15–17], or exhibit Hamming weight symmetry [18, 19].

While these classically affordable studies have provided precious insight into the computing power of AQC, several important mechanisms are yet to be satisfactorily addressed. The general relevance of instantons in AQC [20, 21], and elucidating the many-qubit dynamics of quantum hardware [6] are two examples of largely open problems. Moreover, there are a number of questions which cannot be assessed by equilibrium (or quasi-equilibrium) methods. These include the study of diabatic processes [22]—understood so far only in relatively simple models—and the performances of AQC in finding approximate solutions to large problems, for which the behavior of the success probability with the total annealing time is substantially unknown. Finally, it is known that AQC is a universal computing paradigm only if *non-stoquastic* hamiltonians are considered [23–27]. The latter cannot be studied by traditional simulated quantum annealing and pose a substantial theoretical challenge at the moment [28, 29]. All these points considered, the necessity of new theoretical tools to satisfactorily model, from first principles, AQC on large problems appears particularly urgent.

In this paper, we introduce a variational approach to study AQC in the unitary dynamics setting, and show that it can be used to substantially mitigate the limitations of existing methods. Our approach is based on the time-dependent Variational Monte Carlo method [30, 31], suitably extended to treat time-dependent Hamiltonians. We derive equations of motion enjoying an adiabatic variational principle which guarantees the best unitary adiabatic evolution within the variational manifold. We then demonstrate this approach in a rather wide variety of problems. In particular we show that a simple two-body Jastrow ansatz accurately describes the most common physical scenarios emerging in AQO, such as defect generation through a dynamical phase transition and quantum driving through a frustrated spin-glass phase. Specifically, we first show that a high degree of precision can be obtained in the study of a disordered 1D Ising model. Then we study a fully connected spin glass problem, characterizing the distribution of the success

probability for the quantum algorithm. Finally, we study spin-glass problems on a Chimera graph relevant for existing quantum devices. On those problems, we provide an accurate determination of the statistical properties of genuine AQC on large devices.

II. VARIATIONAL DESCRIPTION

In the AQC protocol, the time evolution of the quantum system is driven by a generic time-dependent Hamiltonian:

$$\mathcal{H}(t) = \Gamma(t; T)\mathcal{H}_f + [1 - \Gamma(t; T)]\mathcal{H}_p, \quad (1)$$

which interpolates, for a total time T , between \mathcal{H}_f , whose ground state should exhibit strong quantum fluctuations in the computational (classical) basis yet be easily prepared, and the problem Hamiltonian \mathcal{H}_p . $\Gamma(t; T)$ is a smooth function such that $\Gamma(t = 0; T) = 1$ and $\Gamma(t = T; T) = 0$. The idea is to prepare the system in the ground state of $\mathcal{H}(0) \equiv \mathcal{H}_f$, and then let the system evolve under the action of the unitary dynamics induced by $\mathcal{H}(t)$. If the evolution is sufficiently slow, then at time $t = T$ the ground state of the problem Hamiltonian $\mathcal{H}(T) \equiv \mathcal{H}_p$ is prepared [11, 32, 33].

As a variational description of this dynamics, we consider a quantum state $|\Psi(\alpha(t))\rangle$, depending on some complex-valued and time-dependent variational parameters $\alpha(t)$. The optimal time evolution of the variational parameters can be obtained using the Dirac-Frenkel time-dependent variational principle [34, 35]. In particular, the variational dynamics lies in an effective low-dimensional Hilbert space spanned by the vectors

$$\langle \sigma^z | O_k \rangle = \frac{\langle \sigma^z | \partial_{\alpha_k} \Psi(\alpha(t)) \rangle}{\langle \sigma^z | \Psi(\alpha(t)) \rangle}, \quad (2)$$

where $\sigma^z \equiv \sigma_1^z, \sigma_2^z, \dots, \sigma_L^z$ is the chosen many-body basis. The variational generator of the dynamics reads

$$F_{\text{var}}(\sigma^z, t) = \frac{d}{dt} \langle \sigma^z | \Psi(\alpha(t)) \rangle \quad (3)$$

$$= \sum_k \dot{\alpha}_k(t) \langle \sigma^z | O_k \rangle \langle \sigma^z | \Psi(\alpha(t)) \rangle, \quad (4)$$

whereas the exact (Schrödinger) generator is

$$F_{\text{ex}}(\sigma^z, t) = -i \langle \sigma^z | \mathcal{H}(t) | \Psi(t) \rangle. \quad (5)$$

The optimal time-evolution can be then obtained upon minimization of the Hilbert-space distance between the variational and the exact generator: $d^2(\dot{\alpha}(t)) = \|F_{\text{var}}(\sigma^z, t) - F_{\text{ex}}(\sigma^z, t)\|^2$. Explicit minimization leads to the following algebraic differential equations for the variational parameters

$$\sum_{k'} \langle O_k^* O_{k'} \rangle_t^c \dot{\alpha}_{k'}(t) = -i \langle \mathcal{H}(t) O_k^* \rangle_t^c, \quad (6)$$

where $\langle AB \rangle_t^c = \langle AB \rangle_t - \langle A \rangle_t \langle B \rangle_t$ indicate connected averages, and $\langle \dots \rangle_t = \frac{\sum_{\sigma^z} |\Psi(\sigma^z, t)|^2 \dots}{\sum_{\sigma^z} |\Psi(\sigma^z, t)|^2}$ are expectation values over the variational state. This approach, in conjunction with an ansatz for correlated wave functions, leads to the time-dependent Variational Monte Carlo (t-VMC) scheme [30, 31], which we adopt here to suitably treat time-dependent Hamiltonians.

A. Variational Adiabatic Principle

A remarkable property of the t-VMC equations, for a time-dependent interpolating Hamiltonian (1), is that they satisfy a type of variational adiabatic principle (VAP). To clarify this point, we introduce the rescaled time $s = t/T$, and observe that the variational equations of motion can be written as

$$\frac{i}{T} \sum_{k'} \langle O_k O_{k'} \rangle_s^c \dot{\alpha}_{k'}(s) = \langle O_k \mathcal{H}(s) \rangle_s^c. \quad (7)$$

In the infinite annealing time limit, the l.h.s. of this equation vanishes provided that: the variational operators O_k are bounded (which is the case for the variational states we consider in the following) and that the variational trajectories $\alpha_k(t)$ are sufficiently smooth, i.e. its time derivatives stay finite during the time evolution. Although the variational state at any time during the evolution cannot be expected to be an eigenstate of the instantaneous Hamiltonian, these two conditions are sufficient to guarantee that it is at least a stationary state within the variational manifold, which represents the closest analogue to an eigenstate available within the constraints of the variational approximation. To see this, observe that the total energy $E(s) = \langle \mathcal{H}(s) \rangle_s$ is stationary if $\partial_{\alpha_k} E(s) = \langle O_k \mathcal{H}(s) \rangle_s^c = 0$, which corresponds to the r.h.s of Eq. (7), vanishing in the adiabatic limit. This VAP holds for any variational state, provided it is evolved according to the t-VMC equations of motion.

III. APPLICATIONS TO ADIABATIC OPTIMIZATION

We now specialize our discussion to one of the most popular applications of AQC, namely adiabatic quantum optimization. In particular we focus on the widely used driving Hamiltonian for computational problems in the Ising form:

$$\mathcal{H}(t) = -\Gamma(t) \sum_i \sigma_i^x + [1 - \Gamma(t)] \sum_{i < j} V_{ij} \sigma_i^z \sigma_j^z \quad (8)$$

where σ_i^α are Pauli matrices, the sums are defined over a certain graph with N nodes, V_{ij} are bond couplings, and $\Gamma(t)$ is a time-varying transverse field, such that $\Gamma(0) = 1$ and $\Gamma(T) = 0$.

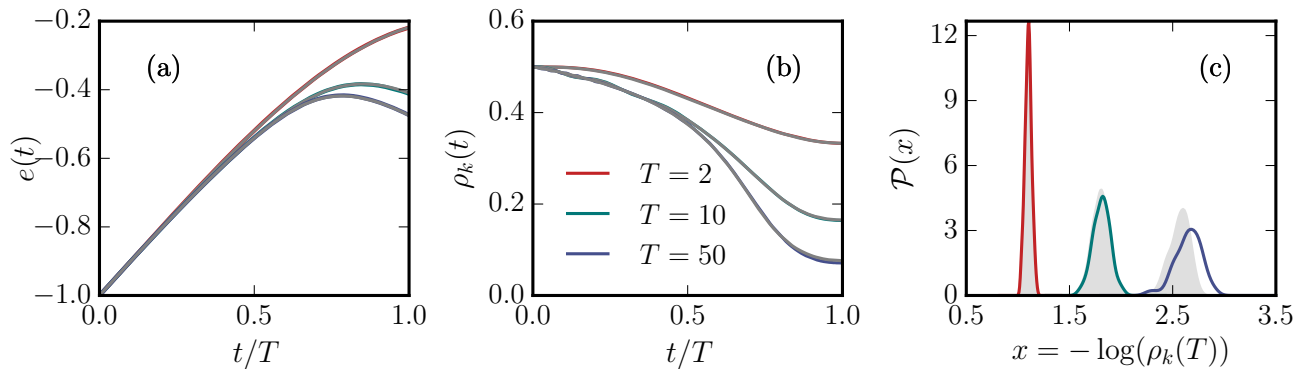


Figure 1. **Variational description of quantum annealing in the disordered 1D Ising model.** Disordered-averaged energy (a) and kinks (b) densities as a function of time t and for several values of the total annealing time T . T-VMC results (in color) are compared to exact ones (gray lines, barely distinguishable). (c) Estimated probability distribution for the logarithm of the kink-density at the end of the annealing, t-VMC results are in color, whereas the exact distribution corresponds to the shaded grey region. All results obtained for a system of $N = 64$ qubits and represent averages over 200 different random couplings.

In order to proceed further, an explicit ansatz for the variational state should also be specified. Since the time-dependent Hamiltonian (8) comprises only few-body interactions, an amenable class of states for the variational adiabatic evolution is the Jastrow-Feenberg expansion (JFE) [36, 37]

$$\Psi(\sigma^z, t) = \exp \left[\sum_i J_i^{(1)} \sigma_i^z + \sum_{i < j} J_{ij}^{(2)}(t) \sigma_i^z \sigma_j^z + \sum_{i < j < k} J_{ijk}^{(3)}(t) \sigma_i^z \sigma_j^z \sigma_k^z + \dots \right], \quad (9)$$

where $J^{(b)}(t)$ are complex-valued variational parameters entangling b spins and the expansions is truncated at some order b_{cut} . This ansatz is exact for the ground state of the Hamiltonian (8) in both limits $t = 0$ (where $J^{(b)}(0) = 0$) and $t = T$ (where the only nonvanishing term is $J_{ij}^{(2)}(T) \propto V_{ij}$). In the following, we will consider the two-body truncated version of this expansion, that is, when we set $J^{(3)} = J^{(4)} \dots = 0$, while keeping one- and two-body terms. As we will demonstrate, for several benchmark cases, this level of truncation is largely sufficient to describe with high accuracy both qualitative and quantitative features of AQCC.

A. Disordered 1D Ising Model

As a first benchmark for our approach, we study a random-bond Ising (RI) model on a 1D lattice. This model is defined by couplings $V_{ij} = -\delta_{i,i+1} v_i$, with uniformly distributed random bonds $v_i \in [0, 1)$. Because we restrict ourselves to nearest-neighbor couplings in one dimension, this model is not frustrated (and remains unfrustrated even when the couplings are chosen with

random signs), and the ground state corresponds to a ferromagnetic configuration with all the spins aligned. Despite the simplicity of the classical ground state, the unitary time evolution induced by Eqn. (8) is known to exhibit a dynamical phase transition through a gapless point in the translationally-invariant case [15]. Furthermore, the disordered model for finite Γ is known to exhibit infinite-randomness phase transitions, which can have exponentially small gaps [38]. This model is therefore a good benchmark for the ability of our scheme to describe nonadiabatic crossings. Another attractive feature of this model is that it can be solved exactly by means of a Jordan-Wigner transformation [15, 16]. Due to the presence of exponentially small gaps, the time evolution, for finite values of the annealing time T , will be typically dominated by diabatic effects. In particular, the density of kinks $\rho_k(t) = \sum_i \langle 1 - \sigma_i^z \sigma_{i+1}^z \rangle_t / (2N)$, which would be vanishing in the exact ground state of the final hamiltonian, instead stays finite during the time evolution and only slowly decreases when increasing T . Moreover, the probability distribution of the kink density at $t = T$ follows a log-normal distribution, which can be understood as a consequence of the gap distribution around the critical point. In Fig. 1 we show the behavior of several quantities of interest for this model, as obtained from our t-VMC approach (color curves) and from the exact solution (gray curves). In Fig. 1-(a), we show the disordered averaged instantaneous energy density $e(t) = \langle \mathcal{H}(t) / N \rangle_t$, in Fig. 1-(b) the disordered-averaged instantaneous density of kinks, and in Fig. 1-(c) the probability distribution of the logarithm of the density of kinks at the end of the annealing ($t = T$). The latter is estimated using a kernel density method for an ensemble of 200 disorder realizations. Overall, the t-VMC approach, in conjunction with the two-body JFE, reaches an impressive level of accuracy. For the shown time-dependent quantities, the discrepancies from the exact results are, indeed, barely visible. Only for the largest annealing time are small

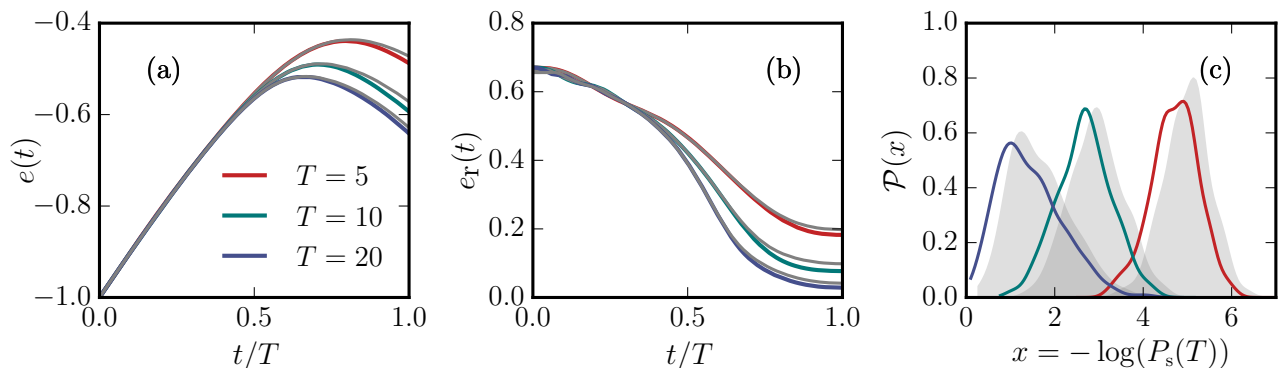


Figure 2. **Variational description of quantum annealing in the Sherrington-Kirkpatrick model.** Disordered-averaged instantaneous energy (a) and residual energy (b) densities as a function of time t and for several values of the total annealing time T . T-VMC results (in color) are compared with the exact ones (gray lines). (c) Estimated success probability at the end of the annealing. The t-VMC results are in color, whereas the exact distribution corresponds to the shaded gray region. All results were obtained for a system of $N = 24$ qubits.

deviations in the kink distribution observed, where the variational approach tends to slightly underestimate the kink density. The high quality of the variational results for this problem suggests the suitability of our approach to describe the complex many-body dynamics of a system going through a dynamical phase transition.

B. Sherrington-Kirkpatrick model

In most optimization problems of interest, couplings V_{ij} can exhibit a high degree of frustration, leading to many solutions of similar energies. To benchmark our approach also in this case, we study spin-glass problems described by the Sherrington-Kirkpatrick (SK) model. The SK model is defined on a fully connected graph, with couplings $V_{ij} = \frac{v_{ij}}{\sqrt{N}}$, where v_{ij} are normal random variates. Unlike the 1d random-bond Ising model, an exact solution for the quantum annealing of the SK model is unknown. In the following, we therefore restrict our benchmarks to relatively small systems, which are still manageable by exact diagonalization. In Fig. 2, we show several quantities of interest, obtained from our t-VMC approach (color curves) and from the exact solution (gray curves). In Fig. 1-(a), we show the instantaneous energy density $e(t) = \langle \mathcal{H}(t)/N \rangle_t$ for a few values of the total annealing time T . In Fig. 1-(b), we show the instantaneous residual energy density $e_r(t) = \langle \mathcal{H}_p/N \rangle_t - e_0$, where e_0 is the ground-state energy of the problem Hamiltonian. We also compute the success probability $P_s(T) = \langle \delta(\sum_{i<j} V_{ij} \sigma_i^z \sigma_j^z - E_{\min}) \rangle_T$ at the end of the annealing, and in Fig. 1-(c) we show the probability distribution (averaged over 500 disorder realizations) of $\log(P_s(T))$ both estimated on the t-VMC results (in color) and on exact results (shaded areas). In contrast to the RI model, we observe some deviations of the variational results from the exact ones. In particular, variational estimates tend to overestimate success proba-

bilities, also resulting in lower average instantaneous energies at finite T . Despite these discrepancies, however, the overall agreement remains very satisfactory and, for example, the variational approach provides a distribution for the success probabilities which is very close to the exact result.

1. Effective temperatures

An intriguing point to analyze in this model is that the two-body-truncated JFE ansatz provides in this case a natural connection with classical annealing. This connection is best understood in terms of the probability density

$$|\Psi(\sigma^z, t)|^2 = \exp \left(2 \sum_{i<j} \text{Re} \left[J_{ij}^{(2)}(t) \right] \sigma_i^z \sigma_j^z \right) \quad (10)$$

which directly maps onto the Boltzmann probability density of a classical system of energy $E_{\text{eff}}(t) = -2 \left(\sum_{i<j} \text{Re} \left[J_{ij}^{(2)}(t) \right] \sigma_i^z \sigma_j^z \right)$. We can then conveniently introduce the time-dependent effective inverse temperatures $\beta_{ij}^{\text{eff}}(t) = -2J_{ij}^{(2)}(t)/V_{ij}$. The conventional approach of classical annealing with time-independent couplings amounts to taking the temperature identical on each bond, i.e. $\beta_{ij}^{\text{eff}}(t) = \beta(t)$ where $\beta(t)$ is an increasing function of time. In the case of quantum annealing, and using this particular ansatz, the above classical description remains possible, but now the effective temperature can exhibit a nontrivial bond-dependent behavior with time. In Fig. 3-(a), we examine this behavior in the distribution (over the bonds ij) of these inverse temperatures at the end of the annealing. These are shown for a single typical instance of the SK model and for some values of the total annealing time T . For small values of T , the effective temperatures follow a very narrow distribution, thus closely imitating the behavior of a simple

classical annealing schedule. As the annealing time is increased, the effective temperatures exhibit a much wider distribution. The very large effective temperatures (in absolute values) encountered for a slow quantum anneal mean that certain bonds are effectively frozen during the annealing procedure. To further elucidate the quantum nature of the annealing, in Fig. 3-(b) we also show the spread of the effective inverse temperatures as a function of time t for a large total annealing time T . In this case, it is possible to appreciate a strong departure from classical annealing, signaled by the lack of a single effective temperature, after a certain *threshold* time (t/T 0.5), as well as the appearance of *negative* effective temperatures.

C. Chimera Graphs

As a further case of study for our approach, we now concentrate on spin-glass problems defined on Chimera graphs (CG). The latter are two-dimensional lattices that can be experimentally realized on the D-Wave quantum annealer. The problems defined on CG have been the subject of several studies, e.g., [39, 40]. However, the majority of previous studies have mainly focused

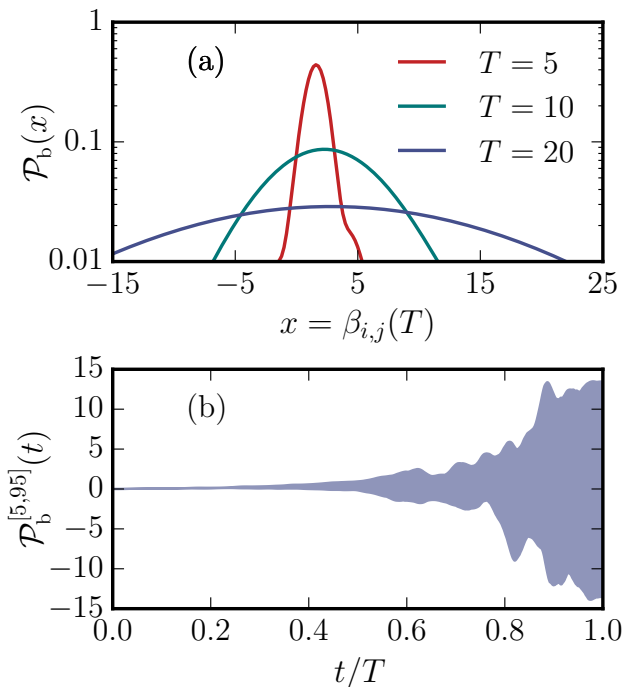


Figure 3. **Effective classical description of quantum annealing in the Sherrington-Kirkpatrick model.** (a) Estimated probability distribution, over the bonds ij , for effective inverse temperature at some fixed disorder realization and for several values of T . (b) Spread of the effective inverse temperature as a function of time, t , at fixed total annealing time $T = 20$. The shaded region is comprised between the 5th and the 95th percentile of the distribution.

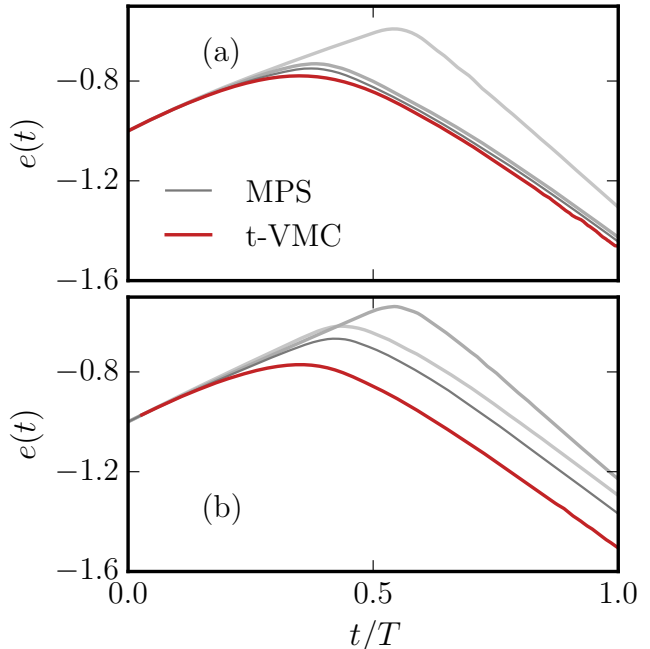


Figure 4. **Comparison with Matrix Product States ansatz for Chimera graphs.** Instantaneous energy density as a function of time t and for a fixed value of the total annealing time T . T-VMC results (in color) are compared to MPS ones (gray lines, with darker colors corresponding to more accurate results obtained with larger bond dimensions $D \in \{8, 16, 32\}$). The number of qubits is $N = 32$ in (a) and $N = 108$ in (b), total annealing time is $T = 24$ in both cases.

on the pseudodynamics of these problems, and little is known at this stage about the physical unitary dynamics for quantum annealings on large CG. To also benchmark our approach in this case, we compare our results to time-dependent matrix-product state (MPS) results [41–44]. The MPS ansatz can be interpreted as a low-entanglement approximation to one-dimensional quantum states and yields an efficient description of the ground states of gapped Hamiltonians in one dimension [45, 46] that exhibit an area law for the entanglement entropy [47]. The approximation can be systematically improved by tuning a parameter referred to as bond dimension, D , which tunes the amount of entanglement that the state can capture.

Although MPS can in principle be applied to higher-dimensional [48] as well as dynamical problems [49–51], the success here becomes limited by the growth of entanglement. In two-dimensional systems, the area law generally leads to exponential scaling of the cost of the MPS description with the linear size of the system. In a dynamical setup, the entanglement can grow up to linearly in time and thus again yield exponential scaling of the cost with time. However, in both cases, numerical experience shows that, in many relevant cases, MPS-

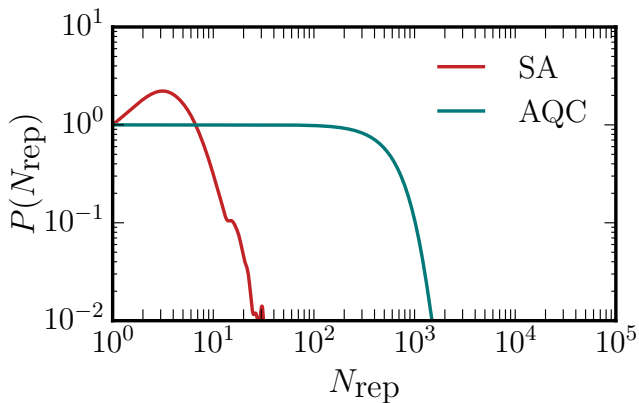


Figure 5. **Probability distribution for the number of repetitions on Chimera graphs.** (Red curve) Classical Simulated Annealing for a number of sweeps $N_s = 1000$. (Right) Adiabatic Quantum Computing at the annealing time $T = 20$. In both cases the probability density is normalized by the value at $N_{\text{rep}} = 1$. The Chimera graph considered has 72 qubits, and 500 disorder realizations have been used to produce the estimates for the probability density.

based simulations using highly optimized codes can outperform exact diagonalization. The setting of adiabatic quantum optimization seems amenable to MPS simulations because both the initial and final states are classical and thus have a simple MPS representation, and furthermore adiabaticity may in some cases limit the growth of entanglement. However, additional complexity arises if the couplings are non-local; for a discussion of this issue, see [52], which also discusses the application of higher-dimensional generalizations of MPS, such as PEPS [53–56], to adiabatic quantum optimization. We note that the variational class of states used in our t-VMC simulations is closely related to complete-graph tensor network states [57, 58].

We perform numerical simulations based on MPS for the smallest non-trivial Chimera graph, which consists of $N = 32$ sites, as well as a larger graph of $N = 108$ sites. In Fig. 4 we show a comparison between the instantaneous energy density obtained by t-VMC (red lines) and by the MPS (where darker curves correspond to more accurate results obtained with increasing bond dimensions). We find that the t-VMC approach yields lower instantaneous and final energies in both cases, compared to the case of MPS with the largest bond dimension we considered here, up to $D = 32$. For a system of 32 qubits, the MPS obtains a good approximation for a bond dimension of $D = 32$. On the largest system with 108 qubits they perform drastically worse when keeping the bond dimension constant, at the same value adopted on the smaller system. This is because mapping the non-planar two-dimensional chimera graph onto a chain leads to a very non-local entanglement structure in this chain, thus requiring an exponentially large bond dimension for an accurate description. We have not attempted scaling the bond dimension beyond the value reported in the text,

and we leave a more systematic analysis to future studies.

1. Efficiency of the adiabatic protocol

A convenient way to characterize the efficiency of the AQC protocol to find the ground state of the spin glass problem is to introduce the average number of repetitions required to obtain the solution with a fixed reference probability p_0 . In particular, we consider $N_{\text{rep}} = \log(1 - p_0) / \log(1 - P_s(T))$, with $p_0 = 0.99$. In Fig. 5 we show the behavior of the probability distribution for N_{rep} at some fixed, typical value of the total annealing time T . In the same Figure, we also show the average number of repetition for classical Simulated Annealing, on the same problems analyzed for the quantum case. The two distributions are qualitatively different. On the one hand, the classical annealing is relatively more compact, while exhibiting a behavior compatible with power-law tails, as found in Ref. [59]. On the other hand, the AQC distribution is substantially more flat, exhibiting a characteristic plateau over several orders of magnitude. While a detailed analysis of the tails is beyond the scope of this paper, we can, however, already see that the behavior of the unitary AQC shows some differences from the SQA one. In particular, the SQA distribution, also analyzed in Ref. [59], does not exhibit the large plateau we observe here. This plateau might therefore be a characteristic trait of the unitary dynamics AQC, as opposed to the quantum Monte Carlo pseudo-dynamics studied until now.

IV. OUTLOOK AND DISCUSSION

We have introduced a variational approach to study the unitary time evolution of interacting spin systems performing a quantum annealing. Several problems previously difficult to study with existing approaches can now be addressed thanks to our variational method. These range from the effect of diabatic transitions to the effort of understanding the possible origins of quantum speed-up. We have shown here how a simple two-body Jastrow ansatz is sufficient to accurately describe most of the properties of interest, when the AQC Hamiltonian involves only few-body interactions. The extension of our approach to study problem Hamiltonians with several-body interactions is feasible, provided that a sensible wave-function ansatz is chosen. A particularly interesting class of variational states is the more recently introduced neural network quantum states [60], which could be used to study AQC in the most challenging applications.

Note Added This work was completed in 2016 and presented at the APS March Meeting in its final form [61]. A preprint with minimal changes was published in 2024.

ACKNOWLEDGMENTS

We acknowledge the discussions with A. Scardicchio, G. Semerjian, D. Venturelli, and F. Zamponi. This work was supported by the European Research Council through ERC Advanced Grant SIMCOFE, by the Swiss National Science Foundation through NCCR QSIT, by Microsoft Research, and by a grant from the Swiss National Supercomputing Centre (CSCS) under project ID

s686. This article is based on work supported in part by ODNI, IARPA via MIT Lincoln Laboratory Air Force Contract No. FA8721-05-C-0002. The views and conclusions contained herein are those of the authors and should not be interpreted as necessarily representing the official policies or endorsements, either expressed or implied, of ODNI, IARPA, or the U.S. Government. The U.S. Government is authorized to reproduce and distribute reprints for Governmental purpose not-withstanding any copyright annotation thereon.

-
- [1] M. A. Nielsen and I. L. Chuang, *Quantum Computation and Quantum Information: 10th Anniversary Edition* (Cambridge University Press, 2010).
- [2] D. Aharonov, W. van Dam, J. Kempe, Z. Landau, S. Lloyd, and O. Regev, Adiabatic Quantum Computation is Equivalent to Standard Quantum Computation, *SIAM J. Comput.* **37**, 166 (2007).
- [3] A. Mizel, D. A. Lidar, and M. Mitchell, Simple Proof of Equivalence between Adiabatic Quantum Computation and the Circuit Model, *Physical Review Letters* **99**, 070502 (2007).
- [4] M. W. Johnson, M. H. S. Amin, S. Gildert, T. Lanting, F. Hamze, N. Dickson, R. Harris, A. J. Berkley, J. Johansson, P. Bunyk, E. M. Chapple, C. Enderud, J. P. Hilton, K. Karimi, E. Ladizinsky, N. Ladizinsky, T. Oh, I. Perminov, C. Rich, M. C. Thom, E. Tolkacheva, C. J. S. Truncik, S. Uchaikin, J. Wang, B. Wilson, and G. Rose, Quantum annealing with manufactured spins, *Nature* **473**, 194 (2011).
- [5] S. Boixo, T. Albash, F. M. Spedalieri, N. Chancellor, and D. A. Lidar, Experimental signature of programmable quantum annealing, *Nature Communications* **4**, 2067 (2013).
- [6] S. Boixo, T. F. Rønnow, S. V. Isakov, Z. Wang, D. Wecker, D. A. Lidar, J. M. Martinis, and M. Troyer, Evidence for quantum annealing with more than one hundred qubits, *Nat Phys* **10**, 218 (2014).
- [7] T. Lanting, A. J. Przybysz, A. Y. Smirnov, F. M. Spedalieri, M. H. Amin, A. J. Berkley, R. Harris, F. Altomare, S. Boixo, P. Bunyk, N. Dickson, C. Enderud, J. P. Hilton, E. Hoskinson, M. W. Johnson, E. Ladizinsky, N. Ladizinsky, R. Neufeld, T. Oh, I. Perminov, C. Rich, M. C. Thom, E. Tolkacheva, S. Uchaikin, A. B. Wilson, and G. Rose, Entanglement in a Quantum Annealing Processor, *Phys. Rev. X* **4**, 021041 (2014).
- [8] A. Douglass, A. D. King, and J. Raymond, Constructing SAT Filters with a Quantum Annealer, in *Theory and Applications of Satisfiability Testing – SAT 2015*, Lecture Notes in Computer Science No. 9340, edited by M. Heule and S. Weaver (Springer International Publishing, 2015) pp. 104–120.
- [9] D. Venturelli, S. Mandrà, S. Knysh, B. O’Gorman, R. Biswas, and V. Smelyanskiy, Quantum Optimization of Fully Connected Spin Glasses, *Phys. Rev. X* **5**, 031040 (2015).
- [10] S. Boixo, V. N. Smelyanskiy, A. Shabani, S. V. Isakov, M. Dykman, V. S. Denchev, M. H. Amin, A. Y. Smirnov, M. Mohseni, and H. Neven, Computational multiqubit tunnelling in programmable quantum annealers, *Nat Commun* **7**, 10327 (2016).
- [11] E. Farhi, J. Goldstone, S. Gutmann, J. Lapan, A. Lundgren, and D. Preda, A Quantum Adiabatic Evolution Algorithm Applied to Random Instances of an NP-Complete Problem, *Science* **292**, 472 (2001).
- [12] G. E. Santoro, R. Martoňák, E. Tosatti, and R. Car, Theory of Quantum Annealing of an Ising Spin Glass, *Science* **295**, 2427 (2002).
- [13] Rønnow, Troels F., Z. Wang, J. Job, S. Boixo, S. V. Isakov, D. Wecker, J. M. Martinis, D. A. Lidar, and M. Troyer, Defining and detecting quantum speedup, *Science* **345**, 420 (2014).
- [14] B. Heim, Rønnow, Troels F., S. V. Isakov, and M. Troyer, Quantum versus classical annealing of Ising spin glasses, *Science* **348**, 215 (2015).
- [15] J. Dziarmaga, Dynamics of a Quantum Phase Transition: Exact Solution of the Quantum Ising Model, *Phys. Rev. Lett.* **95**, 245701 (2005).
- [16] T. Caneva, R. Fazio, and G. E. Santoro, Adiabatic quantum dynamics of a random Ising chain across its quantum critical point, *Phys. Rev. B* **76**, 144427 (2007).
- [17] T. Zanca and G. E. Santoro, Quantum annealing speedup over simulated annealing on random Ising chains, *Phys. Rev. B* **93**, 224431 (2016).
- [18] E. Farhi, J. Goldstone, and S. Gutmann, Quantum Adiabatic Evolution Algorithms versus Simulated Annealing, Preprint (2002), arXiv:quant-ph/0201031.
- [19] L. Kong and E. Crosson, The performance of the quantum adiabatic algorithm on spike Hamiltonians, Preprint (2015), arXiv:1511.06991.
- [20] S. V. Isakov, G. Mazzola, V. N. Smelyanskiy, Z. Jiang, S. Boixo, H. Neven, and M. Troyer, Understanding Quantum Tunneling through Quantum Monte Carlo Simulations, Preprint (2015), arXiv:1510.08057.
- [21] Z. Jiang, V. N. Smelyanskiy, S. V. Isakov, S. Boixo, G. Mazzola, M. Troyer, and H. Neven, Scaling analysis and instantons for thermally-assisted tunneling and Quantum Monte Carlo simulations, arXiv:1603.01293 [quant-ph] (2016), arXiv: 1603.01293.
- [22] S. Muthukrishnan, T. Albash, and D. A. Lidar, Tunneling and Speedup in Quantum Optimization for Permutation-Symmetric Problems, *Phys. Rev. X* **6**, 031010 (2016).
- [23] A. Y. Kitaev, A. Shen, and M. N. Vyalıy, *Classical and Quantum Computation* (American Mathematical Society, 2002).
- [24] M. S. Siu, From quantum circuits to adiabatic algorithms, *Physical Review A* **71**, 062314 (2005).
- [25] J. Kempe, A. Kitaev, and O. Regev, The Complexity of the Local Hamiltonian Problem, *SIAM Journal on Com-*

- puting **35**, 1070 (2006).
- [26] J. D. Biamonte and P. J. Love, Realizable Hamiltonians for universal adiabatic quantum computers, *Physical Review A* **78**, 012352 (2008).
- [27] S. Bravyi and M. Hastings, On complexity of the quantum Ising model, *Communications in Mathematical Physics* **349**, 1 (2017).
- [28] H. Nishimori, Exponential Enhancement of the Efficiency of Quantum Annealing by Non-Stochastic Hamiltonians, arXiv:1609.03785 [quant-ph] (2016).
- [29] L. Hormozi, E. W. Brown, G. Carleo, and M. Troyer, Non-Stoquastic Hamiltonians and Quantum Annealing of Ising Spin Glass, Preprint (2016), arXiv:1609.06558.
- [30] G. Carleo, F. Becca, M. Schiro, and M. Fabrizio, Localization and Glassy Dynamics Of Many-Body Quantum Systems, *Scientific Reports* **2**, 243 (2012).
- [31] G. Carleo, F. Becca, L. Sanchez-Palencia, S. Sorella, and M. Fabrizio, Light-cone effect and supersonic correlations in one- and two-dimensional bosonic superfluids, *Phys. Rev. A* **89**, 031602 (2014).
- [32] T. Kadowaki and H. Nishimori, Quantum annealing in the transverse Ising model, *Phys. Rev. E* **58**, 5355 (1998).
- [33] V. Bapst, L. Foini, F. Krzakala, G. Semerjian, and F. Zamponi, The quantum adiabatic algorithm applied to random optimization problems: The quantum spin glass perspective, *Physics Reports* **523**, 127 (2013).
- [34] P. A. M. Dirac, Note on Exchange Phenomena in the Thomas Atom, *Mathematical Proceedings of the Cambridge Philosophical Society* **26**, 376 (1930).
- [35] Y. I. Frenkel, *Wave Mechanics: Advanced General Theory*, The International series of monographs on nuclear energy: Reactor design physics No. v. 2 (The Clarendon Press, 1934).
- [36] E. Feenberg, *Theory of quantum fluids*, Pure and applied physics (Academic Press, 1969).
- [37] L. Cevolani, G. Carleo, and L. Sanchez-Palencia, Protected quasilocality in quantum systems with long-range interactions, *Physical Review A* **92**, 041603 (2015).
- [38] D. S. Fisher, Phase transitions and singularities in random quantum systems, *Physica A: Statistical Mechanics and its Applications* **263**, 222 (1999).
- [39] S. Okada, M. Ohzeki, M. Terabe, and S. Taguchi, Improving solutions by embedding larger subproblems in a D-Wave quantum annealer, *Scientific Reports* **9**, 2098 (2019), number: 1 Publisher: Nature Publishing Group.
- [40] E. Lobe, L. Schürmann, and T. Stollenwerk, Embedding of complete graphs in broken Chimera graphs, *Quantum Information Processing* **20**, 234 (2021).
- [41] M. Fannes, B. Nachtergaele, and R. F. Werner, Finitely correlated states on quantum spin chains, *Comm. Math. Phys.* **144**, 443 (1992).
- [42] S. R. White, Density matrix formulation for quantum renormalization groups, *Phys. Rev. Lett.* **69**, 2863 (1992).
- [43] S. Östlund and S. Rommer, Thermodynamic limit of density matrix renormalization, *Phys. Rev. Lett.* **75**, 3537 (1995).
- [44] U. Schollwöck, The density-matrix renormalization group in the age of matrix product states, *Annals of Physics* **326**, 96 (2011).
- [45] M. Hastings, Solving gapped Hamiltonians locally, *Phys. Rev. B* **73**, 085115 (2006).
- [46] M. B. Hastings, An area law for one-dimensional quantum systems, *Journal of Statistical Mechanics: Theory and Experiment* **2007**, P08024 (2007).
- [47] J. Eisert, M. Cramer, and M. B. Plenio, *Colloquium* : Area laws for the entanglement entropy, *Rev. Mod. Phys.* **82**, 277 (2010).
- [48] E. Stoudenmire and S. R. White, Studying two-dimensional systems with the density matrix renormalization group, *Annual Review of Condensed Matter Physics* **3**, 111 (2012).
- [49] G. Vidal, Efficient classical simulation of slightly entangled quantum computations, *Phys. Rev. Lett.* **91**, 147902 (2003).
- [50] A. J. Daley, C. Kollath, U. Schollwöck, and G. Vidal, Time-dependent density-matrix renormalization-group using adaptive effective Hilbert spaces, *Journal of Statistical Mechanics: Theory and Experiment* **2004**, P04005 (2004).
- [51] S. R. White and A. E. Feiguin, Real-time evolution using the density matrix renormalization group, *Phys. Rev. Lett.* **93**, 076401 (2004).
- [52] B. Bauer, L. Wang, I. Pizorn, and M. Troyer, Entanglement as a resource in adiabatic quantum optimization, Preprint (2015), arXiv:1501.06914.
- [53] Y. Heida, K. Okunishi, and Y. Akutsu, Numerical renormalization approach to two-dimensional quantum antiferromagnets with valence-bond-solid type ground state, *New Journal of Physics* **1**, 7 (1999).
- [54] T. Nishino, Y. Heida, K. Okunishi, N. Maeshima, Y. Akutsu, and A. Gendiar, Two-Dimensional Tensor Product Variational Formulation, *Progr. Theor. Phys.* **105**, 409 (2001).
- [55] A. Gendiar, N. Maeshima, and T. Nishino, Stable Optimization of a Tensor Product Variational State, *Progr. Theor. Phys.* **110**, 691 (2003).
- [56] F. Verstraete and J. I. Cirac, Renormalization algorithms for Quantum-Many Body Systems in two and higher dimensions, Preprint (2004), arXiv:cond-mat/0407066.
- [57] K. H. Marti, B. Bauer, M. Reiher, M. Troyer, and F. Verstraete, Complete-graph tensor network states: a new fermionic wave function ansatz for molecules, *New Journal of Physics* **12**, 103008 (2010).
- [58] H. J. Changlani, J. M. Kinder, C. J. Umrigar, and G. K.-L. Chan, Approximating strongly correlated wave functions with correlator product states, *Phys. Rev. B* **80**, 245116 (2009).
- [59] D. S. Steiger, T. F. Rønnow, and M. Troyer, Heavy Tails in the Distribution of Time to Solution for Classical and Quantum Annealing, *Phys. Rev. Lett.* **115**, 230501 (2015).
- [60] G. Carleo and M. Troyer, Solving the Quantum Many-Body Problem with Artificial Neural Networks, Preprint (2016), arXiv:1606.02318.
- [61] G. Carleo, B. Bauer, and M. Troyer, Accurate Variational Description of Adiabatic Quantum Optimization (2016), conference Name: APS March Meeting Abstracts.